7.3 ASSIMILATION OF MULTI-SATELLITE HIGH RESOLUTION SEA SURFACE TEMPERATURES FOR A REAL-TIME LOCAL ANALYSIS AND FORECASTING SYSTEM

Corey G. Calvert * and Steven M. Lazarus
Florida Institute of Technology, Melbourne, Florida

Pablo Santos
NOAA/National Weather Service, Miami, Florida

David W. Sharp, Peter Blottman, and Scott Spratt
NOAA/National Weather Service, Melbourne, Florida

1. INTRODUCTION

Much of the significant weather that occurs across the Florida peninsula, especially during the summer, is associated with mesoscale processes (i.e., sea breeze circulation) and their interaction with both the larger scale flow and the coastline (land/water, curvature, etc.). While summer sea breeze-related convection has been studied extensively over the past several decades (e.g., Tripoli and Cotton 1980; Zhong and Takle 1992; Rao et al. 1999, Rao and Fuelberg 2000, Baker et al. 2001, etc.) the impact of the Gulf Stream as it relates to the regional weather has not been fully examined. Deep convection is often observed in the coastal zone (defined here to be within 100 km of the coastline) along a relatively steep horizontal gradient in the sea surface temperature (SST) separating cooler near-shore water along the north and central east Florida coast and the warmer Gulf Stream. The SST gradients are often manifest in visible cloud images during the cool season as surface fluxes vary considerably across the region (e.g., Fig. 1). During the early-to-mid summer, the temperature change across the gradient is on the order of 5°C – which can be comparable to the land/sea thermal contrast.

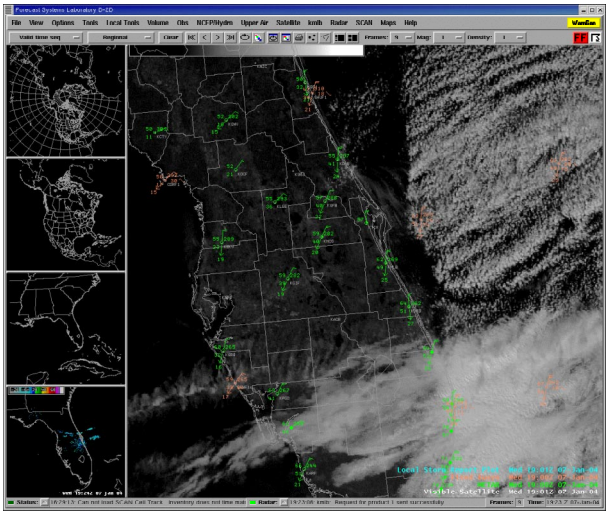

Fig. 1 GOES-E visible satellite image 1900 UTC 7 January 2004. Courtesy of the National Weather Service in Melbourne, FL.

* *Corresponding author address:* Corey G. Calvert, Florida Institute of Technology, Dept. of Marine and Environmental Systems, Melbourne, FL 32901-6975; email: ccalvert@fit.edu

The National Weather Service (NWS) in Melbourne, Florida is cycling the Advanced Regional Prediction System (ARPS) four times per day and its analysis component the ARPS Data Analysis System (ADAS) (run at 15 min. intervals) at a horizontal resolution of 4 km. The model SSTs are initialized using the Real-Time Global Sea Surface Temperature (RTG-SST) analysis provided by the National Centers of Environmental Prediction/Marine Modeling and Analysis Branch (NCEP/MMAB). Generally, the RTG-SST analysis, which has approximately a 50 km horizontal resolution, does not capture the detail associated with the significant offshore SST gradient (compare Fig. 2 and Fig. 3). Because the SST gradients can profoundly impact various aspects of local and regional weather (clouds, precipitation, etc.) we have begun work toward the creation of a real-time 'regional' SST analysis that will downscale the RTG-SST analysis by blending high resolution satellite SST data obtained from both the GOES-12 and Moderate Resolution Imaging Spectroradiometer (MODIS) satellites. The multi-platform high-resolution SST analysis will eventually replace the RTG-SST in the initialization of the NWS Melbourne ARPS/ADAS cycle. Concurrent work associated with preliminary evaluation of the impact of high-resolution SSTs on short-term model forecasts (i.e., on the order of a day) are currently underway in a collaborative effort with the Short-term Prediction and Transition Research Center (SPoRT) in Huntsville, Alabama. We have also had discussions with SPoRT with respect to applying their cloud mask to the MODIS SST data (Haines et al. 2004).

2. DATA

The RTG-SST analysis provides the daily ocean surface temperatures at an approximate horizontal resolution of 50 km and is available once a day from NCEP/MMAB via ftp at polar.ncep.noaa.gov. Each analysis is created on a 0.5º X 0.5º lat/lon grid using a

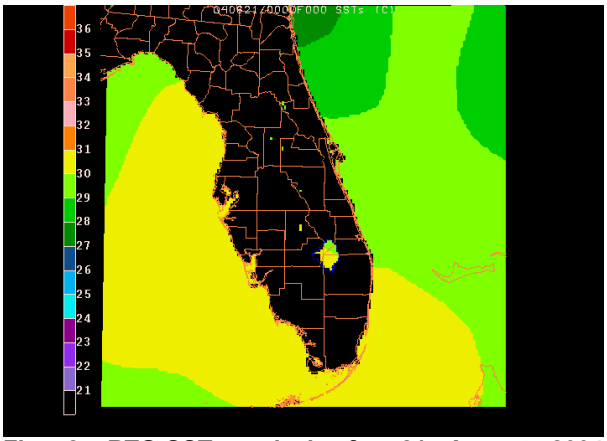

Fig. 2. RTG-SST analysis for 21 August 2004 mapped to the NWS Melbourne ADAS grid.

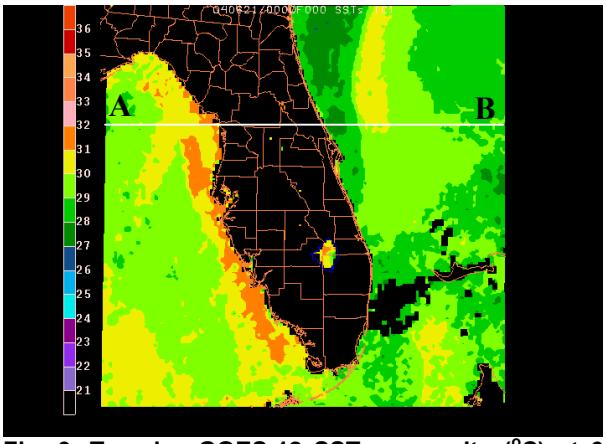

Fig. 3. Two-day GOES-12 SST composite (°C) at 6 km horizontal resolution for 20-21 August 2004 mapped to the NWS Melbourne ADAS grid.

two-dimensional variational (2D-Var) interpolation method that ingests the most recent 24 hours of in-situ observations including buoy and ship data and satellite retrieved SST data (Thiebaux et al. 2001). The high-resolution satellite SST values are averaged over the half-degree grid boxes to create super observations separately for day and night retrievals, however, drifting buoy and ship data are not averaged. Figure 2 depicts a RTG-SST analysis mapped to the NWS Melbourne ADAS domain. Comparison with a similar graphic of a 2-day composite GOES-12 SST map (Fig. 3) indicates that the relatively coarse resolution of the RTG-SST analysis does not accurately capture the narrow SST cold tongue that extends south along the east-central Florida coastline nor the warm coastal waters off the west Florida coast.

The multi-platform approach is attractive in the context of operational meteorology because it takes advantage of the strengths of the various data streams, i.e. the high resolution of the MODIS SSTs and the temporal availability of the GOES-12 data. The GOES-12 SST data, obtained from NOAA/NESDIS in Camp Springs, MD, are available hourly in near-real time (i.e., 3-hour lag) with a horizontal resolution of 6 km. The GOES-12 imager generates SSTs using two channels (3.9 and 11μm). The use of these two channels produces SSTs (in the absence of clouds and sun glint) 24 hours a day at 30-minute intervals. The 30 min. data are combined to produce hourly SST files. Removal of both cloud-contaminated radiances (via a cloud mask) and radiances that are affected by sunglint at 3.9 μm, precede application of the regression-based SST retrieval algorithm (Maturi et al. 2004). The MODIS SSTs are available a maximum of twice daily from both the AQUA and TERRA platforms – and thus have the potential of providing high resolution SSTs within the ADAS domain four times per day. The high spatial resolution (1 km) and real-time availability via direct broadcast from the University of Wisconsin make it an attractive candidate for operational use. Figure 4 depicts the 0700 UTC MODIS SSTs 21 August 2004, which coincides with the RTG and GOES-12 SSTs shown in Figs. 2 and 3. Additional details not evident in the GOES image are captured in the high resolution MODIS image. The demarcation between the Gulf Stream and the cool coastal waters is particularly well resolved as is the eastern edge of the relatively warm Gulf Stream. Because ARPS is run four times per day it is somewhat fortuitous that the MODIS platforms will potentially provide four distinct passes over the ADAS domain each day.

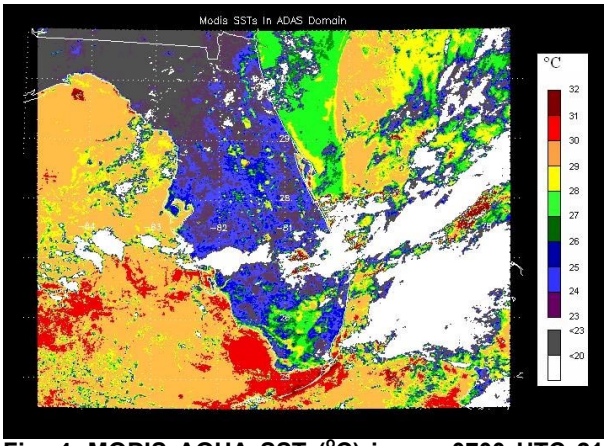

Fig. 4. MODIS AQUA SST (°C) image 0700 UTC 21 August 21 2004. Note that the image is not masked for land or clouds; however, both are easily distinguishable.

3. METHODS

i. NCEP

A collaborative effort with the NCEP Environmental Modeling Center (EMC) during the summer of 2004 has led to the development of an anisotropic 2D-Var assimilation scheme. The analysis is a simplified (i.e. 2D and univariate) version of the new NCEP Gridpoint Statistical Interpolation (GSI) being developed in conjunction with the Weather Research and Forecast model. The anisotropy is general in that it can be 'driven' by gradients in the reference field (e.g., background, terrain, etc.). The correlation function has isotropic and anisotropic components and is specified as

$$\rho(r_1, r_2, f_1, f_2) = \exp(-\left|r_1 - r_2\right|^2 / L^2) \exp(-[f_1 - f_2]^2 / L_a^2) \quad (1)$$

where r_1 - r_2 is the distance between two grid points, f_1-f_2 is the difference between the reference field at the two grid points, and L and L_a are the isotropic and anisotropic scale factors respectively. Small values of L_a cause significant along contour 'stretching' in the presence of large gradients in the reference function (D. Parrish, personal communication).

ii. In House

We are also developing an 'in-house' isotropic 2D-Var algorithm for evaluation purposes using MATLAB version 6.5. The technique minimizes the following quadratic functional:

$$2J(x) = (x - x_b)^T B^{-1} (x - x_b) + \{y_o - H(x)\}^T R^{-1} \{y_o - H(x)\} \quad (2)$$

where x is the control variable (i.e., the analysis after minimization), x_b is the background (i.e., first guess) field, R and B are the observation and background error covariances respectively, y_o are the observations, and H maps the background field to the observation locations. Because we are working with SSTs directly (rather than radiances), H is a bilinear interpolation operator only. Minimization of (2) with respect to the control variable x yields

$$x_a = x_b + (B^{-1} + H^T R^{-1} H)^{-1} H^T R^{-1} \{y_o - H(x_b)\} \quad (3)$$

where x_a is the analysis field (Kalnay 2003). The observation error covariance is defined as a diagonal matrix as we assume that measurement errors made at different locations are uncorrelated. The advantage that the 2D-Var method has over other interpolation schemes is that the many simplifying approximations needed in other methods (e.g. OI) are unnecessary since the objective function (Eq. 2) is minimized using global minimization algorithms (Kalnay 2003). Hence, all data can be used thereby removing the need for data selection that can create erratic solutions at the boundaries of regions that have different observation densities.

4. RESULTS

i. GOES-12 Statistics

To determine the quality, variability, and reliability of the data, we have been producing GOES-12 SST statistics (variance, availability, data latency, etc.) since September 2003. Monthly statistics indicate that the satellite-retrieved SSTs are within about ±0.3ºC of the buoy SSTs during the summer months and within about ±0.5ºC during the winter. However, it is worth pointing out that satellite SST retrievals have been 'tuned' using the buoy SST observations (e.g., McClain et al. 1985) - the latter of which are obtained at a depth of one meter below the ocean surface (compared to a satellite which measures the actual skin temperature). Although attempts are made to correct the bulk versus skin temperature bias, our findings indicate that the buoy SSTs are generally warmer than the GOES-12 SSTs – a finding that is consistent with evaporational cooling at the air-sea interface. In addition to the GOES/buoy comparisons we have also been looking at both the availability and spatial variation of the GOES-12 data. The availability is assessed via the calculation of the percentage of "good" data across the ADAS domain by month. The '% good' is defined as a ratio of the total number of "good" hourly observations (i.e. those that haven't been flagged due to sun glint, clouds, etc.) divided by total number of hours for the month (see Figures 5a and 5b). Examination of approximately a year's worth of data indicates that the availability of the GOES-12 SST data is seasonally dependent with the highest percentages in the summer and fall (generally between 40%-60%, e.g., Figure 5a) and lowest during the winter and spring (10%-40%, e.g., Figure 5b). Obviously data availability is an important issue with respect to operational meteorology and is the primary motivator for the use of a multi-platform approach here. During extended periods of cloud cover the analysis will tend toward the RTG-SST (i.e. climatology). During more favorable conditions (i.e. clear sky) the combination of SST data from two satellite platforms will serve to downscale the RTG-SST analysis.

The spatial variability of the data is also an important statistic because it can potentially serve as a guide for observation error variance estimates. Figures 5c and 5d depict the monthly GOES-12 SST standard deviations for October and December 2003. As one might expect, the variability changes from month-to-month with the largest SST variability in winter and spring. Figure 5c indicates that October SST standard deviations on the order of 0.8ºC with shallow water accounting for the only regions of high variability. In December 2003, the variability is significantly larger across the domain with avg. values ranging from 1.2 to 1.4ºC (figure 5d). The variability is especially high in the areas away from the 'warm' currents such as between the Gulf Stream and the Florida east coast and between the Loop Current and the west coast of Florida.

The availability can also be used to ensure that the variability is a true measure of the temporal variation in the data rather than an artifact of the number of observations. For example, note that Figures 5b and 5d show a region of low data availability over the extreme northeast Gulf of Mexico (GOM, December 2003) that coincides with lower SST variance. Satellite SST retrievals can be contaminated by land and/or strong mixing in the near-shore environment, however, for this case, the low variability is associated with a data drop-off as the number GOES-12 observations over the northeast GOM are limited to the first five days of December 2003.

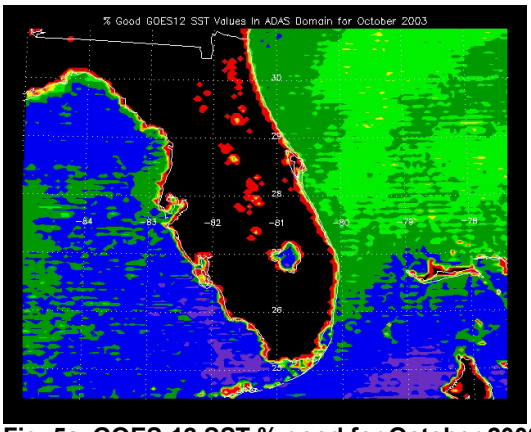

Fig. 5a. GOES-12 SST % good for October 2003.

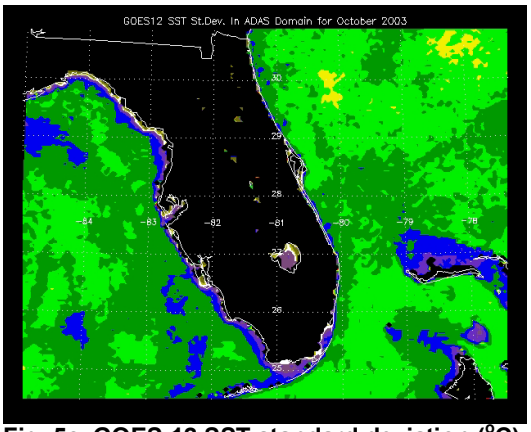

Fig. 5c. GOES-12 SST standard deviation (°C) for October 2003.

(Percentages of good data for 5a and 5b)

0	black	50-60	blue
0-10	crimson	60-70	purple
10-20	orange	70-80	violet
20-30	yellow	80-90	white
30-40	green	90-100	gold
40-50	forest	100	brown

(temps. and st. dev. in degrees Celsius for 5c and 5d)

0	black	1.0-1.2	blue
0.0-0.2	crimson	1.2-1.4	purple
0.2-0.4	orange	1.4-1.6	violet
0.4-0.6	yellow	1.6-1.8	white
0.6-0.8	green	1.8-2.0	gold
0.8-1.0	forest	>2.0	brown

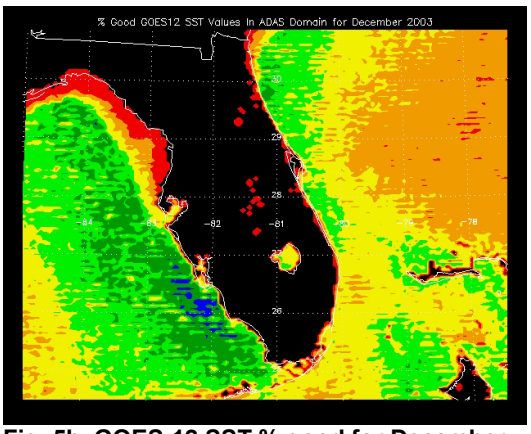

Fig. 5b. GOES-12 SST % good for December 2003.

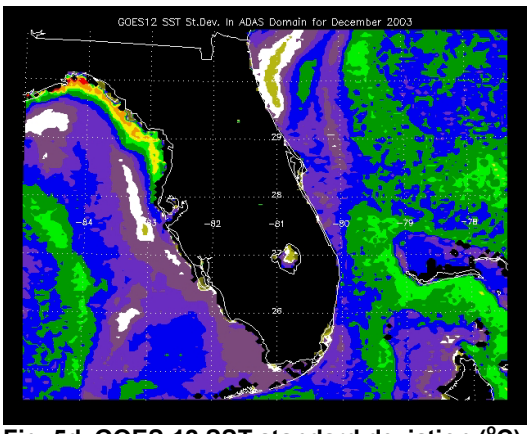

Fig. 5d. GOES-12 SST standard deviation (°C) for December 2003.

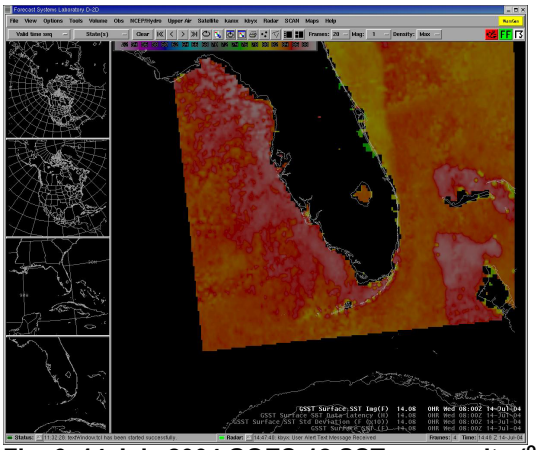

Fig. 6. 14 July 2004 GOES-12 SST composite (°F) as seen on the AWIPS platform.

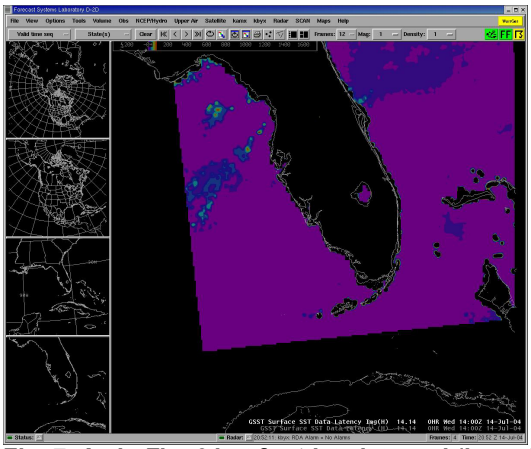

Fig. 7. As in Fig. 6 but for 'data latency' (hours).

ii. GOES-12 Hourly Composites

We are currently providing hourly GOES-12 SST composites to the NWS via the southern region server in both text and NetCDF format. The NetCDF formatted files are being ingested onto the Advanced Weather Interactive Processing System (AWIPS) platform. An example of an SST composite and corresponding data latency image as seen on the AWIPS platform for 14 July 2004 is shown in Figures 6 and 7. Because persistent cloud cover can, at times, lead to SST composites that are unrepresentative, the data latency product is a useful forecasting tool that indicates whether or not the analysis in a given region is current.

iii. 2DVAR

We are performing some simple tests with the in-house 2D-Var scheme and have collapsed it to 1D to examine the impact of the GOES-12 data on the RTG-SST for the 21 August 2004 case shown in Figure 3. The analyses are taken along the west-east cross-section designated by the 'AB' in Figure 3. The analysis is performed directly on the NWS Melbourne ADAS grid (4 km horizontal resolution). Although the 'nearest' GOES-12 observations are offset approximately 2.5 km from the ADAS cross-section, for simplicity we assume that they are collocated (i.e. fall on the cross-section but not necessarily at the ADAS grid points). The RTG-SST is interpolated (bilinear) to the ADAS grid. As expected from Figures 2 and 3, the first guess field (RTG-SST) is quite smooth compared to the observations (GOES-12, see Fig. 8). As previously discussed, the RTG-SST does not capture the warm water off the west coast of Florida (around -83 W) nor the relatively significant cold-to-warm transition just off the east coast of Florida associated with the Gulf Stream.

Three experiments are shown in Figures 8-10. In the first experiment (Fig. 8) we choose a decorrelation length scale of 500 km [i.e., L in Equation (1)] and set the observation-to-background error variance equal to 4 x 10^{-4}. Although the analysis tries to fit the observations – it is quite smooth because we have assumed (erroneously) that data at relatively large distances are correlated. In particular, the analysis has 'jumped' the data gap (i.e., land) in which observations on opposite sides of the peninsula influence the analysis. This obviously produces undesired consequences, i.e., a cooler analysis than the observations support along the west coast (between longitudes –83.5 W and –82.5 W) and warmer analysis than observed along the east coast (between longitudes –81 W and –80 W). In Fig. 9 we set L = 10 km and maintain the same observation-to-background error variance used in the first analysis shown in Fig. 8. As one might expect, the analysis draws tightly to the observations. In Fig. 10 we reverse the error variance ratio (L remains at 10 km) which is now set to 4 (i.e. trust the background field). In this case, the analysis tends toward the RTG-SST. Note that in the absence of observations, for small L, the analysis is reflects the background field (e.g., Fig. 10 between –83 W and –82.5 W).

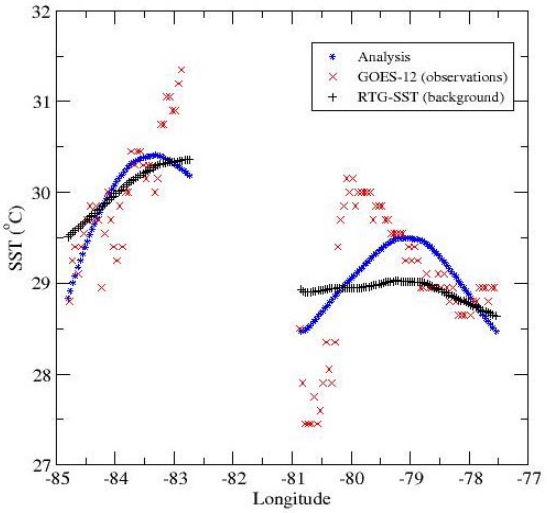

Fig. 8. 1D variational analysis for 21 August 2004 along the E-W ADAS cross-section 'AB' shown in Fig. 3. The various fields are delineated as follows: background/RTG-SST (black plus), GOES-12 observations (red x), and analysis (blue asterisk). See text for more information. Analysis isotropic decorrelation length scale is 500 km and observation-to-background error covariance is 4 x

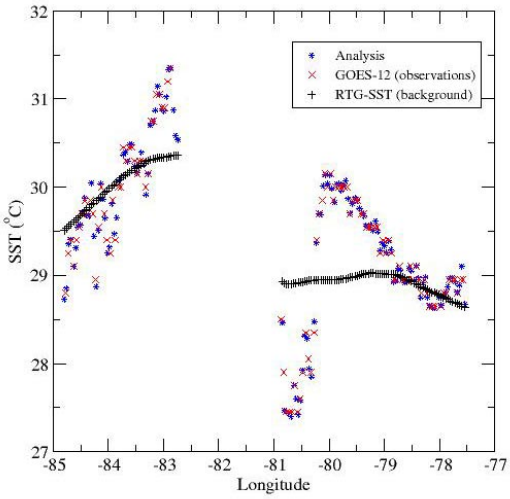

Fig. 9. As in Fig. 8 but for an isotropic decorrelation length scale of 10 km.

5. SUMMARY

The simple 1D variational experiments are instructive and point to some interesting high-resolution analysis issues with respect to data availability, coastline, length scales, etc. In particular, while it is undesirable to apply a large decorrelation length scale, the absence of data (in particular in the near-shore environment) can be problematic as the analysis will tend toward the background in a region where there often appears to be sign-

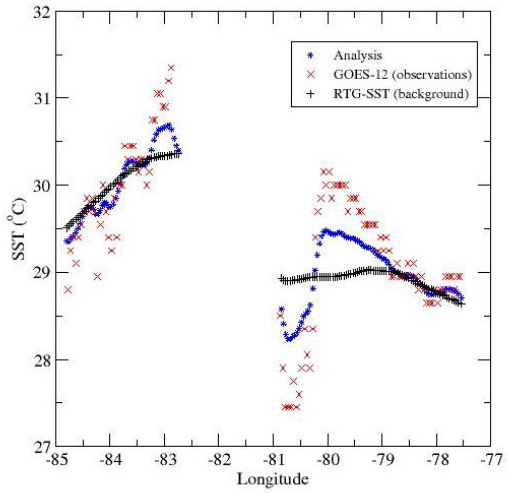

Fig. 10. As in Fig. 9 but for an error variance ratio of 4.

ificant deviations in the high-resolution SST field and the RTG-SST. In part, some of the problems associated with the large decorrelation length scales can be mitigated by introducing anisotropy. In particular, the anisotropy can be driven locally (e.g., in the coastal zone) via a land/water mask which will allow a preferential along shore spreading of information while avoiding the aforementioned pitfalls of the bi-coastal observation influence. These and other issues remain to be resolved in the context of developing a fully operational system to support the short-term forecast and analysis cycle at the NWS Melbourne Forecast Office. We envision an operational SST analysis cycle that is consistent with the NWS Melbourne ADAS/ARPS cycle in which the ARPS is run four times daily.

6. REFERENCES

Baker, R. D., B. H. Lynn, A. Boone, W.-K. Tao, and J. Simpson, 2001: The Influence of Soil Moisture, Coastline Curvature, and Land-Breeze Circulations on Sea-Breeze-Initiated Precipitation. *J. Hydrometeor.*, **2**, 193–211.

Haines S. L., G. J. Jedlovec and F. J. LaFontaine, 2004: Spatially Varying Spectral Thresholds for MODIS Cloud Detection. Preprints, 13th Conference on Satellite Meteorology and Oceanography, Norfolk, VA, Amer. Met. Soc., September 19-23 2004.

Kalnay, E., 2003: *Atmospheric Modeling, Data Assimilation and Predictability*. Cambridge University Press, 341 pp.

Maturi, E., A. Harris, N. Nalli, C. Merchant, S. McCallum, R. Meiggs, and R. Potash, 2004: NOAA's Operational Geostationary Sea Surface Temperature Products. Preprints, *20th International Conference on Interactive Information and Processing Systems for Meteorology, Oceanography, and Hydrology*, Seattle WA., Amer. Met. Soc., January 12-15 2004.

McClain E.P., W.G. Pichel, and C.C. Walton. 1985. Comparative performance of AVHRR-based multichannel sea surface temperature. *J. Geophys. Res.,* **90**, 11585-11601.

Thiébaux, J., E. Rogers, W. Wang, and B. Katz, 2003: A New High-Resolution Blended Real-Time Global Sea Surface Temperature Analysis. *Bull. Amer. Met. Soc.*, **5**, pp. 645–656.

Tripoli, G. J., and W. R. Cotton, 1980: A Numerical Investigation of Several Factors Contributing to the Observed Variable Intensity of Deep Convection over South Florida. *J. Appl. Meteor.,* **9**, 1037–1063.

Rao, P. A., H. E. Fuelberg, and K. K. Droegemeier, 1999: High-Resolution Modeling of the Cape Canaveral Area Land–Water Circulations and Associated Features. *Mon. Wea. Rev.*, **8**, 1808–1821.

Rao, P. A., and H. E. Fuelberg, 2000: An Investigation of Convection behind the Cape Canaveral Sea-Breeze Front. *Mon. Wea. Rev.*, **10**, 3437–3458.

Zhong, S., and E. S. Takle, Eugene S. 1992: An Observational Study of Sea- and Land-Breeze Circulation in an Area of Complex Coastal Heating. *J. Appl. Meteor.*, 12, 1426–1438.